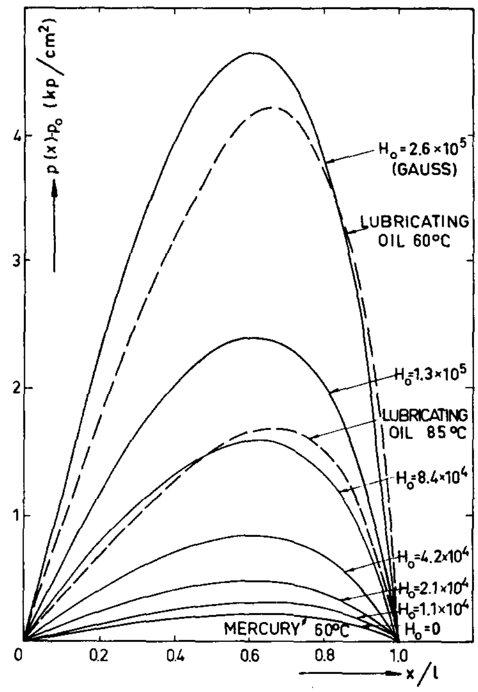

FIG. 2. Pressure distribution over block for mercury depending on H_0 compared with the distribution for lubricating oil at 60° C ($\eta = 0.3$ g cm^{-1} sec^{-1}) and at 85° C ($\eta = 0.12$ g cm^{-1} sec^{-1}).

$$\Delta p(x) = \frac{2\eta M_{\max} U}{a\ \delta^2} \cdot \left[\int_{M_{\max}}^{M(x)} \frac{dM}{M^2 \mathfrak{L}(M)} - \frac{2QM_{\max}}{Ua\ \delta} \int_{M_{\max}}^{M(x)} \frac{dM}{M^3 \mathfrak{L}(M)}\right] \quad (4)$$

if we neglect the small contribution of the induced magnetic field.

We discuss the limit corresponding to the magnetic field going to zero (the purely hydrodynamic bearing). This means that M tends toward zero. With $dM = -(M_{\max}/a)\ dx$ we introduce the variable x and find with

$$\lim_{M\to 0} \mathfrak{L}(M) = -\tfrac{1}{3},$$

$$Q = U\tfrac{1}{2}\delta \frac{\int_0^l (a-x)^{-2}\,dx}{\int_0^l (a-x)^{-3}\,dx}. \quad (5)$$

This is the known hydrodynamic case. Corresponding formulas hold for (1), (2), and (4).

Now we consider the limit corresponding to the angle δ between the walls going to zero. In this case $\frac{1}{2}\delta(a - x)$ goes to L_0 independent of x, from Eq. (3) we find $Q = UL_0$, and with Eq. (2)

$$u(z) = \frac{U}{2}\left[1 - \frac{\sinh\,(Mz/L_0)}{\sinh M}\right]. \quad (6)$$

This is the velocity profile of the known magnetohydrodynamic Couette flow.

For high magnetic fields the relations (3) and (4) read

$$\lim_{M\to\infty} Q = Q_\infty = \tfrac{1}{2}Ua\ \delta \frac{a-l}{l} \ln \frac{a}{a-l} \quad (7)$$

and

$$\lim_{M\to\infty} \Delta p = \frac{\eta UM}{\delta L} \ln\left[\frac{a}{a-x}\left(\frac{a}{a-l}\right)^{-[(a-l)x]/[(a-x)l]}\right]. \quad (8)$$

Equation (4) has been calculated as a function of the magnetic field and the result is shown in Fig. 2. For our numerical example with $a = 20$ cm, $l = 10$ cm, $\delta = 4/3 \times 10^{-3}$, $U = 10^3$ cm sec^{-1}, $\eta = 1.367 \times 10^{-2}$ g cm^{-1} sec^{-1}, $\sigma = 1.1 \times 10^{-5}$ sec cm^{-2} (mercury) we have taken the figures used by Schlichting.[1]

The analysis in detail and the cylindrical case will be treated elsewhere.

[1] O. Reynolds, Phil. Trans. Roy. Soc. London Part I, (1886); H. Schlichting, *Boundary Layer Theory* (Pergamon Press, London, 1955).

Orifice Plates in a Shock Tube

DAVID A. RUSSELL*
Guggenheim Aeronautical Laboratory, California Institute of Technology, Pasadena, California
(Received November 1, 1961)

THIS note points out some interesting aspects of a recent study of the flow resulting from the use of area change near the diaphragm of a shock tube.[1] Earlier studies[2,3] have been directed toward the use of area change for increasing the available shock speed, and thus have considered geometries where $A_4/A_1 > 1$ and $A^*/A_1 = 1$ [see notation on Fig. 1(a)]. In the current work, shock tubes with arbitrary values of these parameters are considered over the complete range of M_s (the shock Mach number).

Neglecting viscous effects, it can be shown that only the four simple wave configurations of Fig. 1 are possible for a shock tube with area change near the diaphragm. A sample set of shock-tube performance curves is presented in Fig. 2, wherein the regions of application of the various configurations are indicated by the lower-case letters corresponding to Fig. 1. Also seen on Fig. 2 are experimental points obtained with the GALCIT 3-in.-square shock tube, using thin orifice plates instead of the contoured nozzles depicted in Fig. 1. Shock-wave attenuation measurements were made, and a simple correction procedure was developed and applied to these points.

It is seen that there is close agreement between the corrected points and the ideal theory, except for a small but systematic discrepancy which occurs for configuration (b). (This discrepancy is seen most clearly for the smaller values of A^*/A_1.) In order to resolve the discrepancy, experiments were made with the $A^*/A_1 = 0.03$ orifice plate replaced by a contoured nozzle, but no difference in shock-tube performance was observed. Next, fine "cold" wires[4] and piezoelectric pressure probes were used in an attempt to try to detect the secondary shock wave of this configuration. Although the secondary expansion wave of configuration (a) was readily detected, the secondary shock wave of configuration (b) could not be observed. Indeed, the wire output was quite different from theoretical predictions based on the ideal-theory model for this case. It became evident that a modified theoretical model was needed to explain the shock-tube behavior over the range of M_s in which this wave had been expected.

Diffuser studies have shown that, owing to boundary-layer interaction, a shock wave may be replaced by a spread-out compression region.[5,6] Assuming this to be the case for the current problem, the simplest new model is obtained by replacing the moving shock wave by a stationary compression, or Fanno-process region. The momentum equation is then replaced by a statement of the pressure ratio across the compression region. This allows for arbitrary frictional processes, and still enables a unique solution to be obtained for the shock-tube performance.

The dashed lines on Fig. 2 represent the performance of such a Fanno-process model. It is seen that this new model resolves the discrepancy between theory and experiment for configuration (b), and that it fairs into the ideal theory for configurations

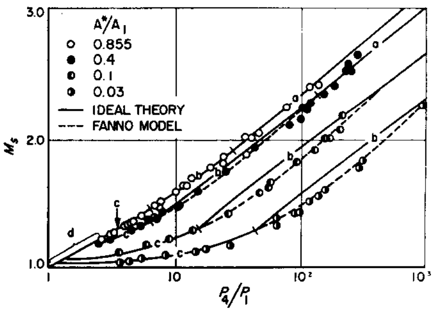

FIG. 2. Nitrogen–air shock tube, $A_4/A_1 = 0.855$ (a, b, c, d correspond to Fig. 1).

(a) and (c). Further, it eliminates the slope discontinuity that had previously existed between configurations (b) and (c), and it was found to explain the observed cold-wire output.

In summary, orifice plates provide good agreement with ideal-theory calculations for all configurations except that in which a nonsteady secondary shock wave is expected. For the latter case, the simple Fanno-process model was found to explain the observed results. The orifice plates are easily constructed and interchanged, and since they can provide a wide range in available M_s for a fixed value of P_4/P_1, they have been found to provide a useful method for controlling the shock Mach number.

The work discussed in this paper was carried out under the sponsorship and with the financial support of the Office, Chief of Ordnance, Army Ballistics Missile Agency, and the Office of Ordnance Research, U. S. Army.

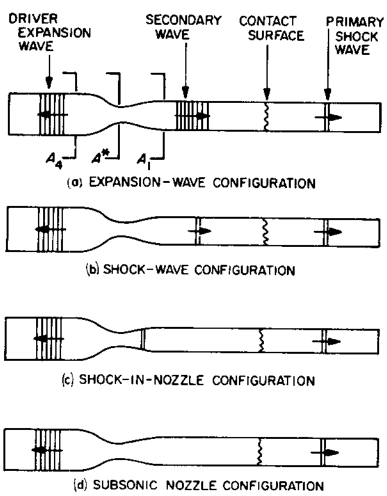

FIG. 1. Schematic shock-tube wave configurations.

* Present address, Jet Propulsion Laboratory, California Institute of Technology, Pasadena, California.

1 D. A. Russell, GALCIT Hypersonic Research Project, Memo. No. 57 (1960).

2 R. A. Alpher and D. R. White, J. Fluid Mech. **3**, 457 (1958).

3 J. Lukasiewicz, "Shock tube theory and application," National Aeronautical Establishment Rept. 15, Ottawa, Canada (1952).

4 W. H. Christiansen, Phys. Fluids **3**, 1027 (1960).

5 H. W. Emmons, *Fundamentals of Gas Dynamics*, Princeton High Speed Aerodynamics and Jet Propulsion Series, Vol. 3 (Princeton University Press, Princeton, New Jersey, 1958).

6 J. Lukasiewicz, J. Aeronaut. Sci. **20**, 617 (1953).

Theory of Nonthermal Ionization in Cesium Discharges

DAVID J. BENDANIEL AND STEPHEN TAMOR
General Electric Research Laboratory, Schenectady, New York
(Received December 11, 1961)

EXPERIMENTAL observation of nonthermal ionization in cesium–helium discharges has recently been described.[1] This note is to report an attempt at constructing a semiquantitative theory